25
Partial Oxidation

Peter Pfeifer

Industrially, hydrogen or synthesis gas is often produced from hydrocarbons via steam reforming (SR):

$$\mathrm{SR}: \mathrm{C}_x\mathrm{H}_y + 2x\mathrm{H}_2\mathrm{O} \rightarrow \left(\frac{y}{2} + 2x\right)\mathrm{H}_2 + x\mathrm{CO}_2 \tag{25.1}$$

Without consideration of microsystems where exothermic processes could be coupled effectively with the SR process, the kinetics, and hence the throughput, are considerably limited by the rate at which the heat can be transferred to the catalytic bed where the endothermic reforming takes place [1]. In most industrial cases, the heat is transferred inside the reactor by non-catalytic partial oxidation (POX) (Equation 25.2) and by autothermal reforming (ATR) (Equation 25.3) in adjacent reaction chambers.

$$\mathrm{POX}: \mathrm{C}_x\mathrm{H}_y + \frac{x}{2}\mathrm{O}_2 \rightarrow \frac{y}{2}\mathrm{H}_2 + x\mathrm{CO} \tag{25.2}$$

$$\mathrm{ATR}: \mathrm{C}_x\mathrm{H}_y + (x-z)\mathrm{H}_2\mathrm{O} + \frac{z}{2}\mathrm{O}_2 \rightarrow \left(\frac{y}{2} + x - z\right)\mathrm{H}_2 + x\mathrm{CO} \tag{25.3}$$

These processes include homogeneous partial or complete oxidation zones at elevated temperatures and are challenges in terms of materials and formation of soot. For POX, the oxygen to carbon ratio is low and the temperature rises to typically 1200–1500 °C [2]. In the case of ATR, oxygen and steam are co-fed and homogeneous combustion is followed by equilibration of the gas on a catalyst fixed bed [3]. The steam addition restricts the combustion temperature and soot formation relative to POX, reduces the oxygen to hydrocarbon ratio, improves the efficiency and increases the H_2 to CO product ratio in the ATR chamber of the reactor. Because of these advantages, ATR has been implemented successfully in large syngas plants in recent years [4]. The temperature gradients are, however, still large and the transfer of heat from exothermic to endothermic reaction zones is facilitated mainly by convection.

Micro Process Engineering, Vol. 2: Devices, Reactions and Applications.
Edited by V. Hessel, A. Renken, J.C. Schouten, and J.-I. Yoshida

ISBN: 978-3-527-31550-5

25.1
Distinction Between Catalytic and Industrial Processes

Reduced temperatures at high throughput could be obtained through catalytic partial oxidation (CPO), oxygen-assisted, so-called catalytic oxidative steam reforming (OSR) or catalytic autothermal steam reforming (CAR). This nomenclature was chosen to distinguish in the following sections between the POX/ATR industrial process and novel catalytic short contact time processes for syngas production found in the literature. Analogous to the POX process, the CPO process is strongly exothermic under stoichiometric conditions and produces more heat than necessary. This makes it difficult to control the temperature increase and profile in conventional fixed-bed catalysts and thus to anticipate the syngas selectivity in relation to process parameters [5]. At the entrance of the reactor, total oxidation could be the predominant mechanism for the temperature increase, whereas at a sufficient residence time, a water gas shift (WGS) or SR reaction can proceed with water and CO_2 both formed by total oxidation. At elevated temperatures, homogeneous reactions can also compete with catalytic processes, such as dehydrogenation or cracking. To avoid the total oxidation or side-reactions leading to oxygenates or alkenes at elevated catalyst temperatures, steam can be added (OSR). By this means the thermodynamics are shifted to higher hydrogen yields. The CAR process can be seen as a special case of OSR leading to a balance of heat loss to the environment, heat consumption by the endothermic reactions and heat generation from exothermic reactions taking place in one reaction chamber.

Attention to these processes by microprocess engineers has resulted in the CPO and OSR having much faster kinetics than the steam reforming process. Avoiding huge outer reactor dimensions as in the case of steam reforming, the OSR has possible advantages in terms of costs for microfabrication, application and process intensification. Weight and size reduction could enhance portable hydrogen generators for fuel cell applications. The huge heat transfer capacity of the microstructure can be seen as a possible solution for achieving heat transfer from oxidation zones to reforming and WGS zones along the reactor length (axial heat distribution) and thus increasing process efficiency. Depending on the microstructure design and philosophy, additional heat removal or heat distribution with cooling media can further enhance the advantages of the microstructured device.

The following sections deal with recent research carried out in a microstructured environment with respect to catalysts, reactor concepts and process parameters from pure CPO to CAR via OSR.

25.2
Catalysts

Depending on the philosophy of the microdesign, the microstructure itself can be seen as a catalyst support or solely as a reactor wall. The catalytically active species can be used as raw material for microfabrication or can be deposited by conventional

methods such as incipient wetness impregnation or chemical vapor deposition directly on the microstructure wall or on an additional support, which would be integrated into the microstructure. In the following sections investigations in so-called millisecond-contact time reactors [6] such as monoliths and foams are also included in the considerations of catalyst design. These reactor types are close to the definition of "real" microsystems in terms of characteristic dimensions of the internal structure. Cordierite monoliths, for example, can be fabricated with channel diameters down to less than 1 mm; metallic honeycombs for exhaust gas treatment in automotive applications are available with channel widths down to approximately 600 μm and foam pores can be produced in almost the whole micrometer range. The catalyst interaction with the reactor walls, the gas-phase contributions and heat and mass transfer of these systems can thus be very similar.

25.2.1 Catalytically Active Species

Irrespective of the reactant type, the most prominent catalytically active materials found for microstructured environments are noble metals since they offer the highest turnover rates and fastest kinetics at high selectivity. As mentioned earlier, fast kinetics of the catalysts can be the determining factor for the economic success of the microsystem.

From the wide range of noble metals, the use of rhodium in coatings and catalytic layers or integrated in the microstructure was proven to be a good choice for the conversion of alkanes such as methane [7–10], propane [11–14], octane [15, 16], decane [16, 17] and hexadecane [16], for alcohols such as methanol [18, 19], ethanol [18] and propanol [18], for mixtures such as gasoline [20] and for aromatic compounds such as naphthalene [16]. In the literature, there is little doubt about the considerable contribution of the direct steam reforming route to CO_2 and hydrogen for OSR and the high activity for the WGS reaction on rhodium.

A different approach could be the use of platinum, experimentally investigated by researchers for methane [21, 22], ethane [23, 24], propane [24], decane [17], methanol [19, 25], ethanol [26] and gasoline [21]. Mechanistic investigations, however, revealed a high decomposition activity to form CO coupled with low WGS activity [24], leading to a lower hydrogen yield on platinum than on rhodium. Furthermore, the incomplete dissociation of larger compounds such as decane is considered to be responsible for the decrease in catalytic surface area, leading to lower activity of platinum compared with rhodium [17].

Little work can be found in the literature on the conversion of methane by other noble metals such as palladium and ruthenium. Palladium was investigated for methane [27] and ethanol CPO [26] but with little success for high conversion. Ruthenium was investigated for ethanol CPO and showed comparatively good activity [28].

Among non-noble metals, the industrially well-known nickel system has been investigated by only a few researchers for ethanol [29] and isooctane CPO [30]. Conclusions for this catalytically active species were that the catalyst system should be

improved [29] and that at the high space velocities applied in the microreactor, the nickel system yielded modest conversions (60–75%). In other cases, attempts were made to increase the yield of methane CPO on nickel by coupling two sequential monoliths, one coated with combustion catalyst and another with nickel for subsequent steam reforming and WGS [31]. However, the total methane conversion did not exceed 92%, even with platinum as a precombustion catalyst.

An exception in terms of catalysts is the catalytic partial oxidation or OSR of methanol due to the low reaction temperature required. Copper [25, 32–36] and palladium–zinc alloy [36–38] have been proven to give high selectivities and space–time yields. For the latter system, the palladium forms an alloy with the zinc oxide support under reducing conditions above 300 °C and is stable under the reaction conditions of methanol steam reforming [39]. However, the stability of the alloy under CPO has not been proven so far by X-ray diffraction after exposure to reaction conditions.

25.2.2 Catalytic Supports and Promoters

Major issues in steam reforming and catalytic partial oxidation or catalytic oxidative steam reforming are oxygen storage and the acidity of the catalyst support, which could be relevant in terms of soot or alkene formation.

For the methanol CPO, this issue is less important due to the low reaction temperature and thus the promoting effects of the support are even more favorable. Analogous to methanol synthesis, ZnO is considered [25, 33–35] to be effective for both issues, namely the increase and stabilization of copper surface area and increase in turnover rates on copper. Special cases of the supported copper system are the use of leached brass wires [34] (Figure 25.1a) and the sintering of dendritic copper powder together with Cu/ZnO catalyst [35] (Figure 25.1b) to form the reactor microstructure.

Other supports for copper mentioned in the literature are chromium oxides [32, 33] and zirconium oxide [33], which were found to possess a higher activity for the OSR and higher CO_2 selectivity compared with the zinc oxide-supported copper system, respectively.

For the methanol OSR on palladium in fixed-bed reactors, the use of ZnO seems to be necessary [37, 38] to yield high reforming and WGS activity, whereas decomposition is observed predominantly on zirconium oxide supports [37].

For higher reaction temperatures such as for alkane, alkene and ethanol CPO and OSR, the issues of oxygen storage and low acidity are addressed irrespective of the catalytically active species by the use of cerium oxide [18, 20, 21, 26] or α-alumina [11–14, 18, 19] as supports, respectively. From propane CPO and OSR investigations on rhodium deposited on Fecralloy microstructured metallic monoliths [11, 12, 40], which segregates α-alumina during annealing (1000 °C) prior to impregnation or on α-alumina foams [13, 14], it is known that soot formation is negligible under normal working conditions of CPO and OSR. For the conversion of alcohols, a comparison of rhodium on α-alumina monoliths and on an additional cerium oxide support for rhodium on the same monoliths revealed less byproducts

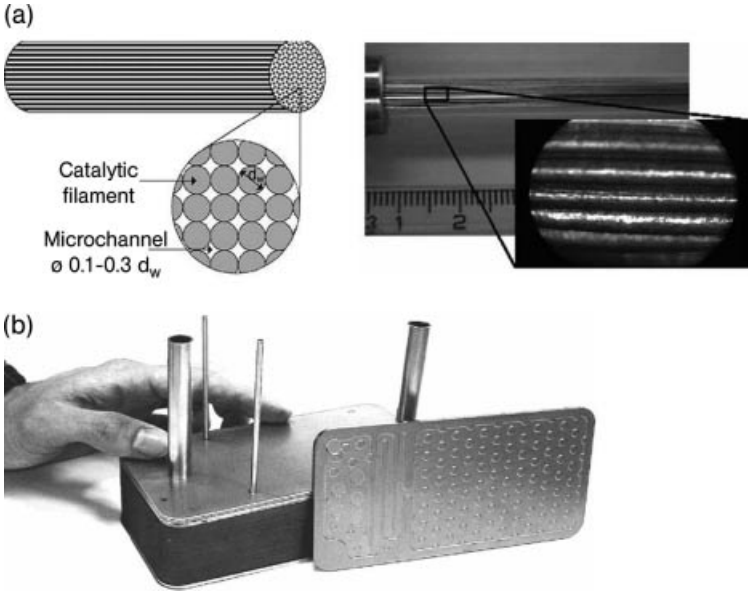

Figure 25.1 (a) Leached brass wires inside a quartz tube [34] and (b) stacking of porous layers of catalyst to form the microstructured reactor [35].

such as oxygenates and alkenes on the latter support. This is suggested to be due to rapid consumption of all oxygen in the rhodium/α-alumina catalyst leading to homogeneous side-reactions [18]. Hence to inhibit homogeneous reactions, the size reduction of the pore or channel system seems also to be an important factor for the selectivity.

Despite the above-mentioned advantages of cerium oxide and α-alumina especially for the conversion of alcohols, a wide variety of investigations have dealt with alkene conversion on γ-alumina-supported active species [16, 28, 41]. For sol–gel layers, which can also be used as a support for CPO [8], the determination of the aluminum phase is often not reported (e.g. [42]) as calcination temperatures between 300 and 700 °C could result in a considerable contribution of amorphous phases to gamma phases and at 800–1000 °C there is an additional transition to a delta phase [43].

Recent research in packed beds [38], ceramic monoliths [20] and microreactors [30] also revealed an excellent performance of a Ce–Zr support mixture, which was explained by an increase in surface area by the addition of zirconium oxide [38]. A zirconium oxide-supported rhodium catalyst also revealed similar ignition performance to a mixed Ce–Zr oxide supported rhodium catalyst on the surface of Fecralloy monoliths with trapezoidal channels [9]. A novel route to a support, which might be useful for CPO and OSR, is the synthesis of silicon carbide foam, recently used for steam reforming [44] (Figure 25.2). This support would also be less acidic and is suitable for building a compact foam catalyst.

An important factor for selectivity can be the microstructured material, for example when catalytically active species or supports are deposited on metals. Even

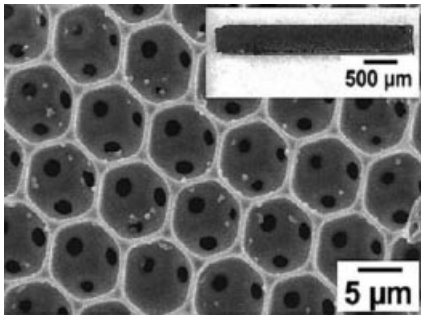

Figure 25.2 Silicon carbide foam as catalytic support [44]. Inset: an optical micrograph of an entire SiC porous monolith.

though the homogeneous reaction is completed at temperatures as high as 1700 °C in porous systems [45], gas-phase reactions can lead to considerable soot formation induced by metallic walls containing, for example, nickel. Depending on the wall distance, not only the microstructured region [18] but also the design and material of the outlet or inlet regions could be an important factor for ignition prior to the catalyst section [11] or inside the reactor outlet.

25.3 Reactor Design and Results

There are different possibilities for expressing distinctions between the reactor systems which can be found in the literature. In the case of CPO and OSR, it is reasonable to make distinctions between:

(a) the use of catalytic packed beds and foams in metal/silicon microstructures
(b) the use of catalytic walls.

For catalytic wall systems, a further distinction is the following:

(b1) the use of microstructured catalytic active material
(b2) the deposition of catalytically active species on microstructure walls
(b3) the deposition of catalytically active species on additional catalyst supports.

Sometimes the distinction between (a) and (b2)/(b3) appears very difficult at first sight, as the idea of foams or pressed catalyst powder integrated into micro-/millimeter sized gaps or microchannels is very similar to a foam body in terms of catalyst preparation. However, this additional distinction is used for the reactor design rather than the catalyst preparation.

Irrespective of the above distinction, another difference among the reactor designs is the heat management, i.e. the use of single microchannels and the use of parallel microchannels or microstructures. In most cases the single microchannel operated, for example, in a furnace or in a heating block, leads to nearly isothermal reactor

operation through heat dissipation by a high solid volume to reaction volume ratio present in a single microchannel arrangement. Independent of CPO, OSR or CAR mode, the multichannel systems without adjacent cooling microstructures could result in nearly adiabatic reactor control depending on the system size and insulation. When the number of microchannels is small, the reactor could be operated in a transition between adiabatic and polytrophic modes, which should be avoided in terms of reactor control. Due to considerable heat losses through the outer walls in systems with internal microstructure of less than several cubic centimeters, high heat conductivity of the microstructure diminishes the radial temperature gradient and thus the polytrophic contribution. For investigations in multichannel systems in the laboratory, where economic aspects of heat are often negligible, it is reasonable to prevent large temperature gradients to the environment and thus polytrophic contributions by heat shielding, for example by electrical heating of the reactor inside a circular gold mirror (radiative) or by electrical heating of a thin outer insulation around the reactor (conductive). This was performed, for example, in the catalytic partial oxidation of methane [7] and in the CPO and OSR of propane [11–14] in small microchannel monoliths and foams. Data obtained with negligible polytrophic contributions can be transferred directly to industrial applications by using additional parallel microstructures inside a reactor housing ("equal-up").

25.3.1
Packed Beds and Foams in Microstructures

Single-channel packed beds were used, for example, for the catalytic partial oxidation of methane [8, 10, 27]. In all cases the reactor designs have been developed mainly for the determination of the kinetics of fast exothermic reactions. However, different heating concepts have been used.

Reactors fabricated by deep reactive ion etching (DRIE) possessed a very high silicon to reaction volume ratio and were resistively heated to compensate for high heat loss. Heating was accomplished with a piece of silicon on top of the channel [27] or with a nickel disilicide strip integrated below the channel gaining access to the reaction zone covered by Pyrex glass [8]. Even though the catalyst was prepared by the sol–gel technique, the catalyst loading obtained by several subsequent coating steps was so high in both cases that nearly the whole channel was filled similarly to a packed bed (Figure 25.3). Conversion of methane was up to 90% at 650 °C and the H_2 : CO ratio was in the range from 2.1 to 2.5 depending on the oxygen to carbon (O_2:C) ratio from 0.66 to 0.25, respectively. Ignition of the CPO reaction was observed at around 550 °C.

In the other case [10], the reactor consisted of a 1 mm diameter quartz glass capillary with a 20 µm wall thickness. A 15 mm length of capillary was filled with 2.5 wt.% rhodium on alumina powder obtained by flame spray synthesis and was inserted in a hot gas flow perpendicular to the capillary. With this setup, it was possible to evaluate the oxidation state of rhodium by applying a small X-ray beam. Different absorptions on rhodium species have been detected with a positive

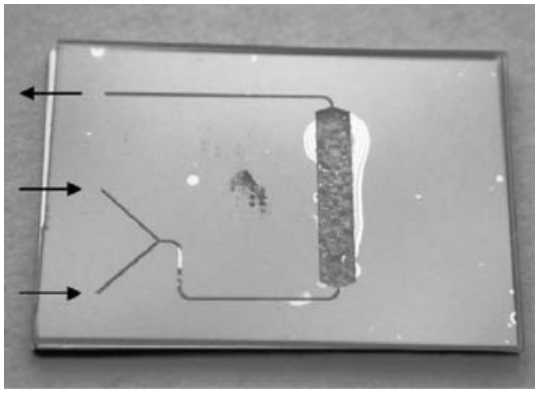

Figure 25.3 Single-channel microreactor covered with Pyrex glass (heating element not visible) filled with 0.1 wt.% rhodium on alumina [8].

sensitive X-ray camera (Figure 25.4). The results were obtained for an O_2 : C ratio of 0.5 and in the temperature range 338–378 °C for methane CPO.

Coated foams have been integrated for co-heating the steam reforming of natural gas by the catalytic partial oxidation of natural gas in adjacent microsized slits for easy scale-up for offshore synthesis gas production and subsequent Fischer–Tropsch or methanol synthesis [46]. The catalyst was solution coated on a 40 pores cm^{-1} foam and inserted in 640 µm slits. No information was given on the catalytically active species used. The conversion which was given exceeded 95%. However, this is the value yielded after combustion of the produced synthesis gas (exhaust).

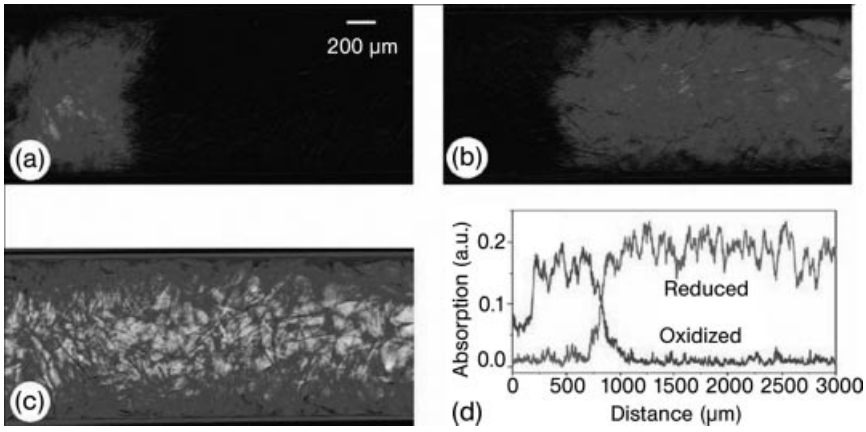

Figure 25.4 (a) Oxidized Rh species (light); (b) reduced Rh species (light); (c) featureless background; (d) relative concentration of the oxidized (increasing with distance) and reduced (decreasing with distance) Rh particles in the axis of the fixed bed. Conditions: 362 °C, space velocity $1.9 \times 10^5\ h^{-1}$ [10].

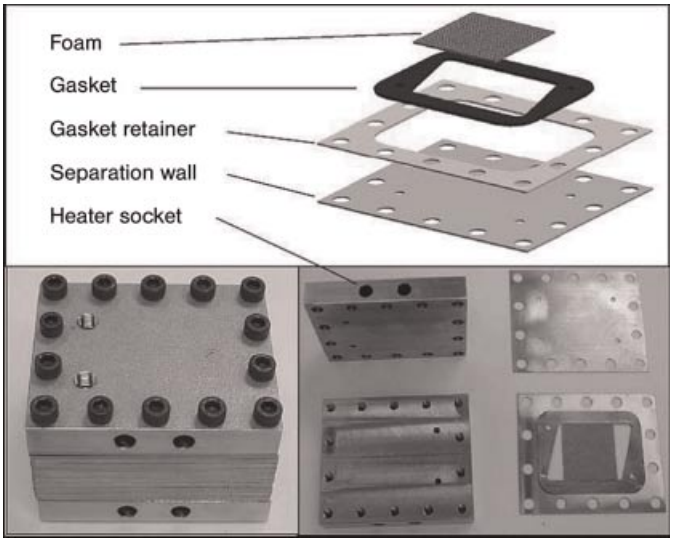

Figure 25.5 Sketch/exploded view of the layer assembly (top), mounted reactor (left) and photograph of the individual reactor parts (right) [30].

Detailed descriptions of the reactor layout and results were given for the CAR of isooctane [30]. The nickel catalyst was deposited on Fecralloy foam supported by a mixed cerium–zirconium oxide layer. The coprecipitate consisted of $Ce_{0.75}Zr_{0.25}O_2$ and was impregnated with aqueous solution to yield 10 wt.% nickel. The foam was sealed with a gasket between separation walls and heated between two heater sockets (Figure 25.5). The maximum conversion of isooctane in this assembly was 75% at near 700 °C. A steam to carbon ratio of 2, an O_2:C ratio of 0.5 and much higher space velocities [gas hourly space velocity (GHSV) $5.6 \times 10^5\,h^{-1}$] were applied for the microreactor in comparison with the fixed bed, which was investigated in the same study.

25.3.2
Catalytic Wall Reactors

25.3.2.1 Microstructured Catalytically Active Materials

Two systems of structured catalytically active materials have been shown already in Section 25.2.2 (Figure 25.1). On leached brass wires [34], the conversion of methanol was dependent on the procedure of surface treatment and the leaching fluid. Brass of different composition leached in 3.7% HCl or 10% NaOH followed by subsequent calcination at 600 °C and reduction at 250 °C showed nearly no conversion, whereas the same treatment with aluminum-coated brass wires showed good activity under steam reforming conditions. Basic leached catalyst deactivated rapidly. The number of results for CPO and OSR presented in this study was fairly limited. The hydrogen yield and methanol conversion reached approximately 80% and 60%, respectively, at

245 °C for CPO and 60% and 35%, respectively, at 320 °C for OSR. The ignition temperature for the OSR at a steam to carbon ratio of 1.2 and O_2 to methanol ratio of 0.3 was approximately 250 °C.

In the case of the sintered mixture of dendritic copper and Cu/ZnO catalyst powder [35] forming the reactor walls, the final reactor design included vaporization, CAR of methanol and selective CO oxidation for CO reduction in the presence of hydrogen (Figure 25.6). For the vaporization and selective CO oxidation, the sintered metal was additionally coated with platinum. The outlet flow of the reactor consisted of 40% hydrogen, 20% CO_2, 0.1% CO and residues of 1.2% methanol (dry basis, balance N_2) at a steam to carbon ratio of 1.

A similar approach for building microchannels from catalytically active material is the "modified ceramic tape casting" process [21]; 0.5 wt.% Pd/CeO_2 was, for example, dispersed in xylenes and alcohols (dispersion and solvent agent), cast at a desirable thickness with fugitive materials incorporated and dried. The dried material possesses flexibility due to the organic binders and can therefore be cut and rolled. Fugitive materials can be burned subsequently to yield the microchannels. By this technique, microchannels or gaps between rolled layers of down to 1 µm can be fabricated (for rolled material, see Figure 25.7). The microchannels obtained from

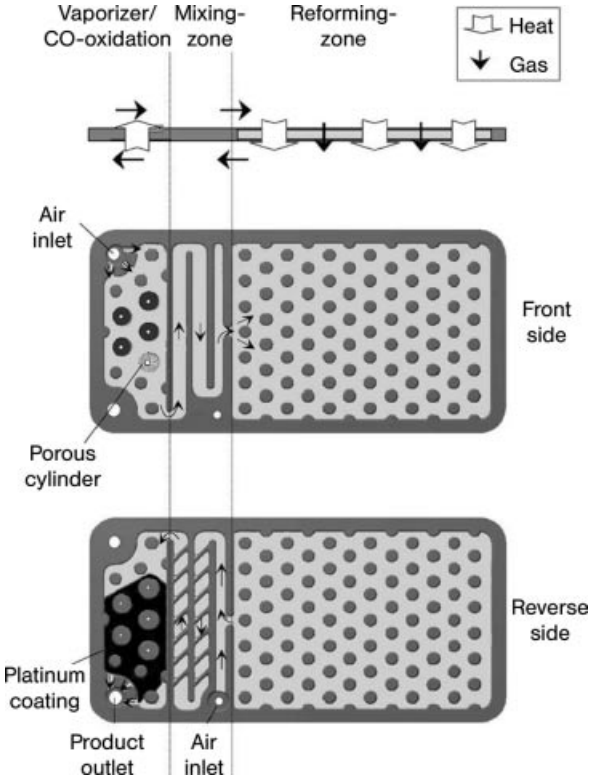

Figure 25.6 Cross-section, top and bottom views of a sintered mixture of dendritic copper and Cu/ZnO catalyst [35].

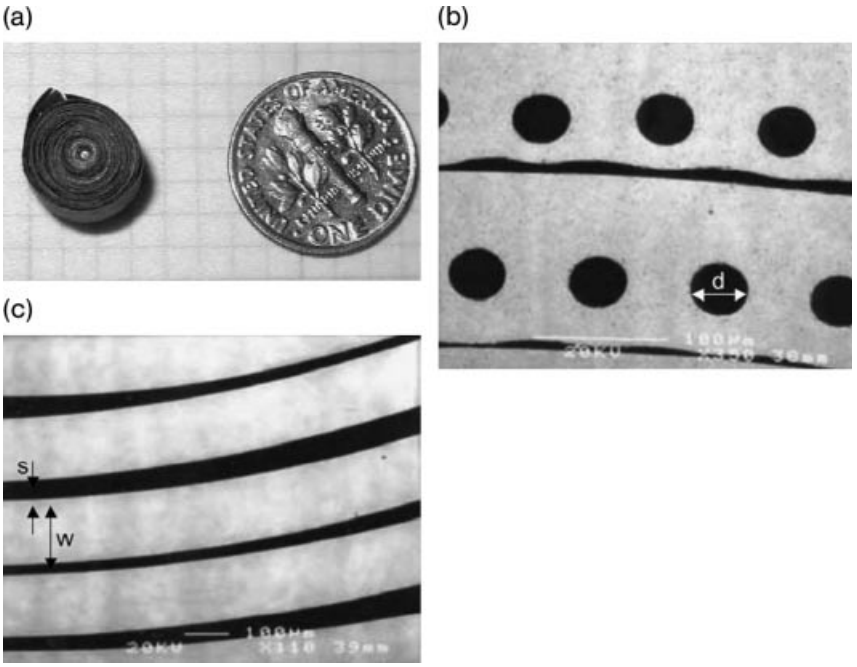

Figure 25.7 (a) Rolled material from the "ceramic tape casting" process; (b) channels (diameter *d*) produced by integration of fugitive fibers; (c) gaps (s) by integration of fugitive strips [21].

this process were tested for OSR of isooctane under conditions of an O_2 to isooctane ratio of 3.7, a water to isooctane ratio of 9.1 and a GHSV of $2.5 \times 10^5\,h^{-1}$ with approximately 90% hydrogen selectivity.

A different approach to yield a microstructure out of catalytically active material was the micromachining of rhodium foils to build up a metallic monolith [7]. Different monoliths have been fabricated with channels of depth 108–131 µm, width 60–120 µm and length 5–20 mm by stacking and welding of the structured foils. Using heat shielding via a surrounding ceramic body (Figure 25.8), the reactor was operated at low thermal gradients. Taking into account the experimental error of less than ±25 K for the applied pyrometer, 50–120 K differences between reactor inlet and outlet and no radial gradients were measured in the monoliths for methane CPO. At very high temperatures, for example 1100 °C, the conversion rates on the longest monolith reached 90% methane conversion and 88% hydrogen yield. The GHSV applied to the monoliths was in the region of $0.2 \times 10^6\,h^{-1}$ on a structured volume basis. The free channel volume was around 30% inside this structured volume.

25.3.2.2 **Deposition of Catalytically Active Species on Microstructure Walls**

On ceramic monoliths, foams or metallic microchannels, catalytically active species can be deposited directly on the structured wall, when the microstructure already

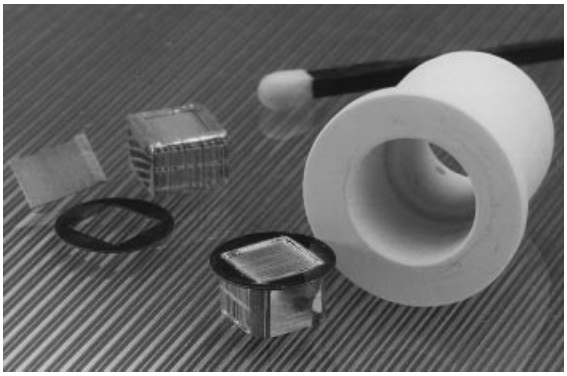

Figure 25.8 Structured foil, foil stack and orifice, welded foil stack with orifice and ceramic heat shield (electrically heated by a resistant heating wire surrounding the ceramic body) [7].

supplies a high surface to volume ratio. For metals this issue is critical when the catalytically active species can diffuse into the material in the reduced state. Therefore, it could be necessary to pretreat the metal. This can be done by annealing to yield an oxide layer, which would act like a diffusion barrier.

Direct impregnation of α-alumina monoliths was performed in several cases [17–19]. For methanol CPO, platinum and rhodium were used at 2 and 2.4 wt.% loading on 45 pores per inch (ppi) monoliths, respectively [19]. The coated monoliths, 17 mm in diameter and 10 mm long with 45 ppi, exhibited a light-off temperature around 150 °C and showed few differences in terms of catalytic behavior. Platinum showed a 5% lower CO_2 selectivity, correspondingly higher CO selectivity and slightly higher selectivity for methane than rhodium in addition to no reactivity to form alkenes at methanol to O_2 ratios of 2–6.

A wider variety of alcohols [18] and alkenes [17] were investigated under CPO conditions on platinum- and rhodium-coated monoliths with 5 wt.% of catalytically active species. The results obtained with monoliths having the same dimensions as for methanol CPO revealed that a small surface area of active species can lead to higher alkene selectivity by homogeneous reactions. Platinum was also judged to be unable to dissociate higher alkenes completely. Thus, an increase in catalytically active surface area by means of a washcoat or a reduction in the channel size can lead to a higher H_2 yield.

Alumina foams have been directly impregnated for propane CPO and OSR [13, 14, 40] to yield 0.01 wt.% rhodium. The catalyst on the foam body, which was 15 mm in diameter, 7 mm long and contained 400 cells per square inch (84% porosity), showed optimum performance at an oven temperature of 700 °C and good stability under CPO conditions (C:O = 0.8), even though a remaining hot spot of more than 200 K was observed in the foam. Under OSR conditions (C:O = 0.5 and steam to carbon ratio = 1) only a 150 K hot spot was observed. However, the catalyst deactivated more rapidly, maybe due to the increase in byproduct formation. Complete homogeneous conversion was observed at an oven temperature of 800 °C

with uncoated foam. More details of the experimental results can be found in Section 25.4.

Direct impregnation of metallic structures was performed in other studies for CPO and OSR of propane [11, 12, 40]. Rhodium was deposited on annealed Fecralloy monoliths. Annealing leads to segregation of α-alumina at 1000 °C and thus gives a small increase in surface area. The monoliths, which were 20 mm long with cross-sections of 5.5 × 5.6 mm and possessed roughly 600 channels of 120 × 120 μm, were impregnated with 1 mg of rhodium. Tests were performed with different setups, heat shielding according to Figure 25.7 or with a gold-plated mirror with internal radiation heating (Figure 25.9). The reaction temperatures in this study were measured along the middle of the reactor axis. It was found in the metallic monolith that the temperature gradients were as low as 150 and 100 K for CPO and OSR, respectively. Also, the catalyst did not deactivate over several months of conducting tests. More results from this study will be presented in the Section 25.4. in comparison with foams.

25.3.2.3 Deposition of Catalytically Active Species on Additional Catalyst Supports

The geometric design of the ceramic monoliths used for additional catalyst supports is not very different from that used for direct deposition of catalytically active species. The idea, however, of applying a washcoat or oxide support prepared by wet impregnation (e.g. [16, 20, 31, 33]) is to increase the surface area, to modify the pore structure or to modify the support interaction with catalytically active species. The additional functionalization with cerium oxide can, for example, suppress alkene and oxygenate formation by inhibiting complete oxygen consumption in the catalytically active species and thus homogeneous reactions [17]. The addition of a γ-alumina washcoat can increase the surface area of catalytically active species and thus suppress homogeneous reactions [18].

One approach to reactors with additional supports is the use of metallic monoliths with trapezoidal channels of 1.2 mm hydraulic diameter for methane CPO for "catalytically rich combustion" in a gas turbine [9]. Fuel is turned partly into hydrogen before combustion. The catalyst was Rh/ZrO_2 coated on a Fecralloy monolith.

The concept of a single annular duct yielding a low pressure drop can also be used for coating with additional supports such as γ- or α-alumina. This was applied, for example, for CPO of light alkanes using platinum and rhodium catalytically active species [24].

For foams the approach of additional catalyst support is the same as for monoliths. This is especially necessary when using metal gauzes, which can be arranged like foams in multiple layers. This produces a higher heat and mass transfer by smaller boundary layers compared with conventional monoliths [41]. A comparison of monoliths and such gauzes is shown in Figure 25.10. An arrangement of the metal gauze can be as screens as in Figure 25.10a (applied for methane CPO on a γ-alumina washcoat with rhodium as catalytically active species [41]) or as cylindrical coils for radial flow as in Figure 25.10b (applied for OSR of methanol on Pt, Pd or Rh deposited on an alumina washcoat [48]). Results have been promising here; for example, process selectivity of CPO was 93% on reducing the peak temperatures in the gauze arrangement to less than 1100 °C at nearly full conversion [41].

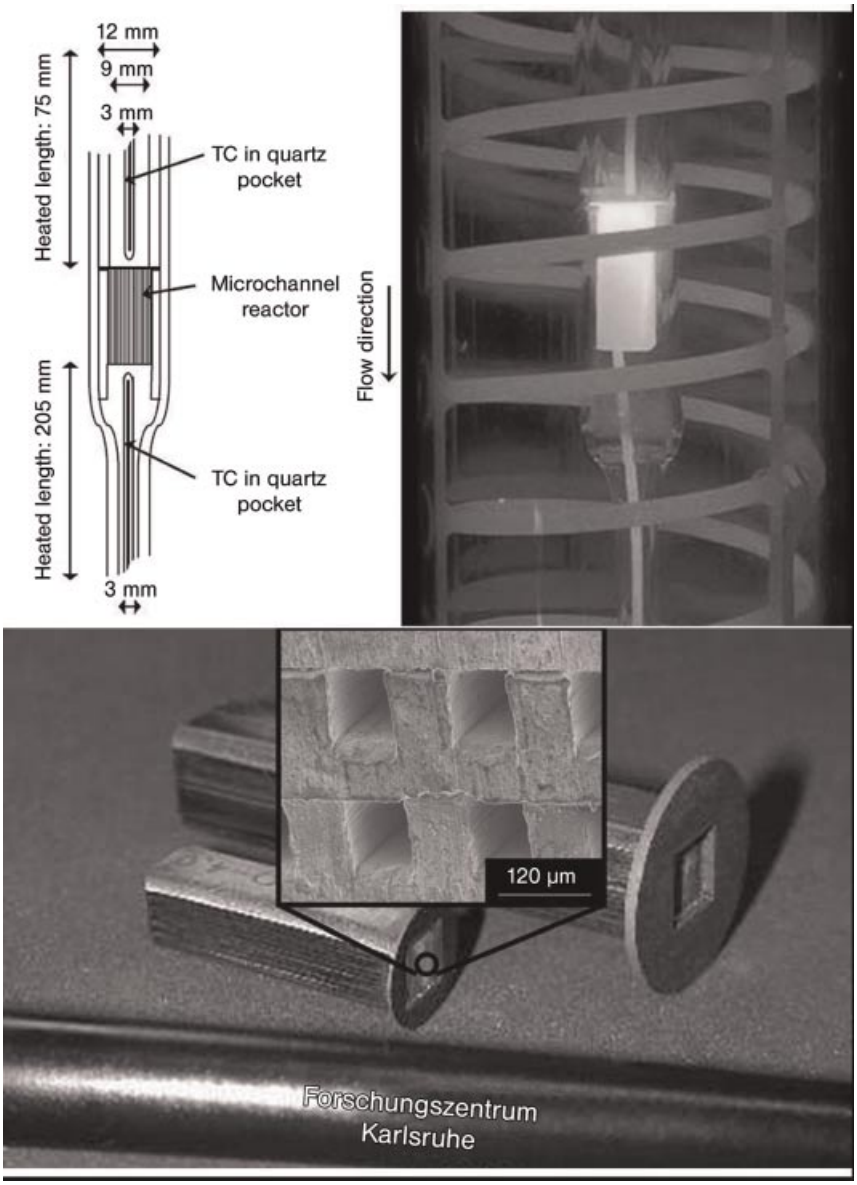

Figure 25.9 Scheme of the reactor housing (left) and photograph (middle) of the heat-shielded reactor under operation (gold mirror becomes transparent) [40] and different reactor sizes (right; inset: magnification of microchannel structure) [47].

Microstructured metals have recently been coated by the sol–gel technique to obtain a Cu–Zn–Al catalyst system or by the emulsion colloid technique, which is similar to a standard washcoating procedure, to obtain a PdZn/ZnO catalyst system

(a)

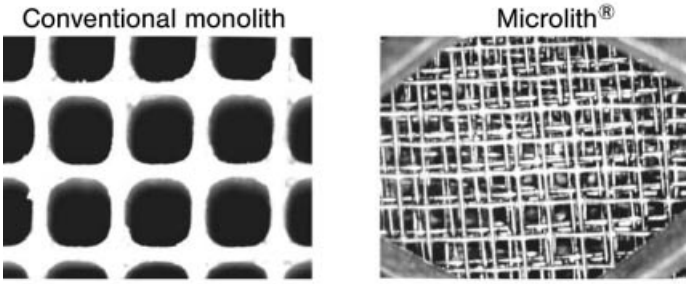

60	Cells (cm^2)	400
2.64	Geometric surface area ($m^2\ L^{-1}$)	6.3
7-10	Channel length (cm)	0.007
70-120	Channel length to diameter ratio (L/d)	0.3
1050-1200	Operating temperature (°C)	105-1200
70	Frontal open area (%)	72

(b)

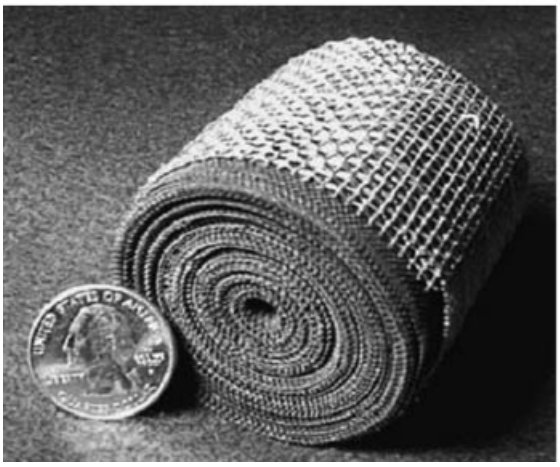

Figure 25.10 (a) Physical characteristics of conventional monolith and Microlith substrates [41]; (b) rolled Microlith material for radial flow from the center [48].

for the OSR of methanol [36] (Figure 25.11a). For the latter system, the coating looked fairly uniform; however, it peeled off very easily so that all catalytic tests were performed with the copper system. At an O_2 to methanol ratio of 0.3 and a steam to methanol ratio of 1.2, the results on the copper catalyst system were promising. Nearly full conversion and high WGS activity (low CO content) at GHSV up to $1.5 \times 10^4\,h^{-1}$ and reaction temperatures of 600 °C were reached.

A similar approach was adopted on single microstructured metal foils covered in a metal housing for catalyst screening during CPO of propane [49]. Platinum, palladium and rhodium on a γ-alumina washcoat catalysts were used, with the best

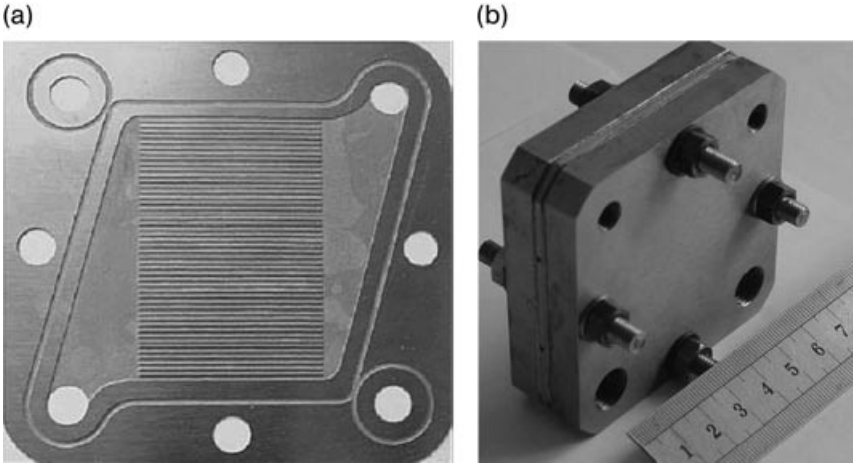

Figure 25.11 Microchannel plate design (left) and mounted microchannel reactor (right) for methanol OSR [36].

results for the rhodium system. In this study, however, the coking of the metal tubing made from stainless steel determined the operation time and is thus under further investigation.

25.4 Reactor Comparison

"Is the use of microstructured devices necessary?" That is one of the most important questions for the use of microstructured reactors. Of course, the answer is not trivial because different parameters can be determining in different applications. Determining parameters could be size, weight, catalyst amount, dynamic behavior or the cost, including subsequent or earlier process steps for hydrogen generation from CPO or OSR. Another issue is that none of the research results have been adapted to the industrial scale and subsequently validated under industrial practice. Even though fast start-up, high catalyst efficiency and sometimes also weight comparisons have been reported in the literature, the final answer will be found in the future.

Different issues also arise for the comparison of different reactors. Furthermore, data in the literature are often not comparable. This is why only reactor comparisons from the literature will be indicated exemplarily in the following text.

For example, "modified ceramic tape casting" catalysts are reported to be twice as active for isooctane OSR as pellet catalysts of the same type and amount under the same feed composition [21].

A similar conclusion of superior performance of structured reactors was drawn from the CPO of ethanol in a comparison of foams, ceramic monoliths and pellets [28, 29]. However, it was stated that the pellets showed good activity and selectivity but poor suitability for mobile applications. In further comparisons of the

foams and monoliths, the foams exhibited slightly higher selectivity and activity due to a larger pore size and higher tortuosity.

A comparison between ceramic foams and metallic microstructured monoliths of Fecralloy was performed for the OSR and CPO of propane under similar conditions of total catalyst amount, catalyst composition and modified catalyst residence time [40]. A major difference in this investigation was, however, that uncoated foam was located before and after the catalytically coated foam to prevent gas-phase ignition. Irrespective of this difference, two main conclusions can be drawn: first, the catalyst supported on the microchannel structure did not deactivate like the foam catalyst under OSR conditions. This could be due to the fact that peak temperature

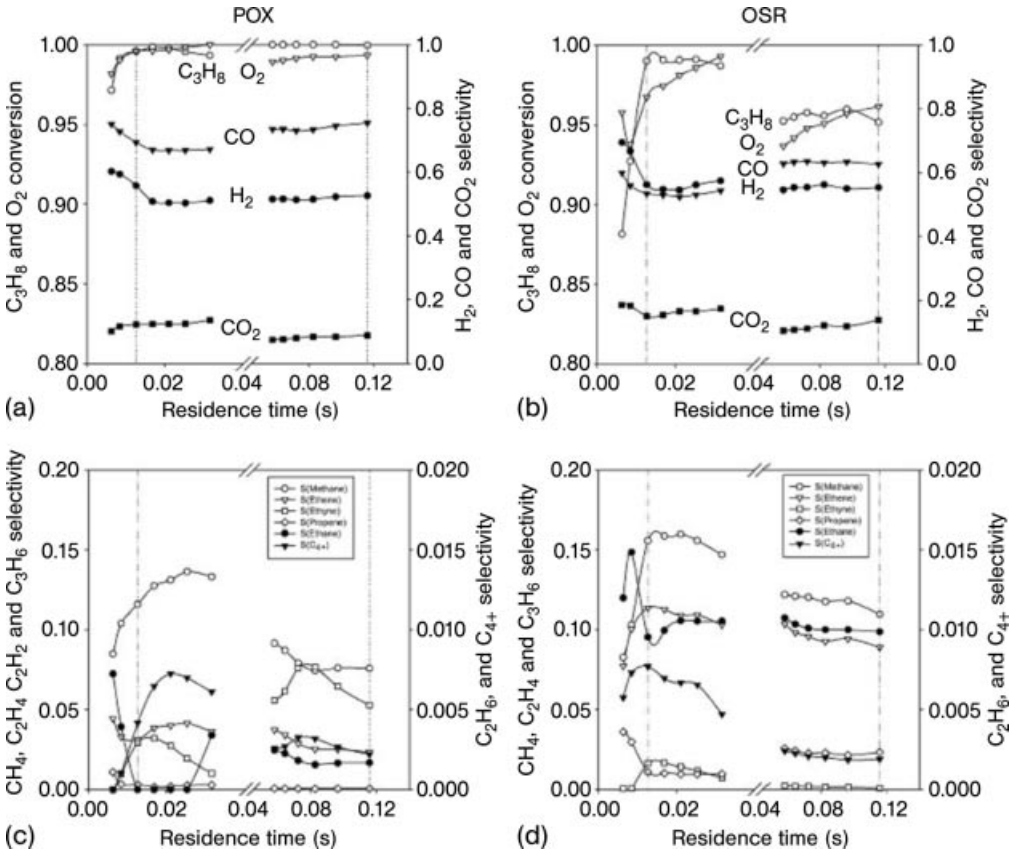

Figure 25.12 Conversion and selectivity to main products (a and b) and by-products (c and d) as a function of residence time during CPO (a and c) and OSR (b and d). The left-hand series in each diagram represents experiments over the 1.0 mg Rh/Al_2O_3/Fecralloy microchannel monoliths for a total reactant flow of 400–2000 mL min^{-1} STP and a furnace temperature of 800 °C. The right-and series in each diagram represents experiments over 0.25 mg Rh/Al_2O_3 foams for a total reactant flow of 1000–2000 mL min^{-1} STP and a furnace temperature of 700 °C. The vertical lines indicate total reactant flows of 1000 mL min^{-1} STP [40].

differences were 50–100 K less in the microchannels than in the foams. Second, the reaction temperature needed was lower for the foams, maybe due to the higher peak temperature. Product compositions at furnace temperatures of 700 °C for the foams and 800 °C for the microchannels, conditions which could provide a good reactor comparison, were, however, overlaid by gas-phase ignition before the microchannels and thus exhibited an increasing number of byproducts (Figure 25.12). At very low residence times of approximately 0.01 s this can be suppressed by quenching at high total flow, seen from the rapid decrease in byproducts. However, the gas-phase contribution might not be negligible and thus needs further study with uncoated foams before and after the metallic monolith.

The comparison of metallic monoliths directly fabricated by micromachining of rhodium and of rhodium deposited on micromachined Fecralloy monoliths exhibited superior WGS activity and thus higher hydrogen yield for the deposited rhodium system [12]. This could be explained by the higher surface area of rhodium on the additional alumina support on Fecralloy prepared by annealing at 1000 °C.

25.5 Conclusion

For catalytic partial oxidation or oxidative steam reforming no additional heat supply is necessary for self-sustaining operation of the hydrogen production unit. In cases where dilution of the produced hydrogen due to use of air as oxidant is not critical, these process routes yield more compact reactors than steam reforming due to faster reaction kinetics. Fast heat supply like in the case of steam reformers is also not necessary for achieving fast startup of reactors, but microreactors can, however, provide significant advantages due to improved heat and mass transfer for obtaining higher selectivities, space time yield and catalyst lifetime as compared to conventional fixed bed reactors. This is correlated with decrease of hot-spot temperatures due to good heat conductivity of the structured catalyst system. Heat can be transferred within the catalyst to zones where reforming processes are proceeding and the reduction of hot-spots avoids total oxidation. Improved mass transfer to the catalytic sites can also prevent gas phase reactions which are supposed to increase olefin side products.

The approaches found in literature for preparing the catalyst are ranging from packed bed microreactors to catalytic wall reactors. Catalytic walls can again be provided by different approaches, so that a wide variety of different reactor designs has been investigated so far. In the majority of reactors noble metals are used as catalyst, since the turnover numbers on these metals are quite high compared to other systems like nickel. High turnover numbers are also beneficial to obtain small and compact hydrogen production systems and by increasing compactness the high heat and mass transfer coefficients of microreactors get even more important. On the other hand, highly active catalyst and microreactors should be combined since both systems might be more costly than conventional reactors.

References

1 W. Balthasar, D. J. Hambleton, *Int. J. Hydrogen Energy* **1980**, *5*, 21.

2 M. H. Eikani,Canadian Patent Application, CA 2428339, **2004**.

3 J. R. Rostrup-Nielsen, *Catal. Today* **1993**, *18*, 305.

4 K. Aasberg-Petersen, J.-H. Bak Hansen, T. S. Christensen, I. Dybkjaer, P. S. Christensen, C. Stub Nielsen, S. E. L. Winter Madsen, J. R. Rostrup-Nielsen, *Appl. Catal. A* **2001**, *221*, 379.

5 T. Ioannides, X. E. Verykios, *Catal. Lett.* **1997**, *47*, 183.

6 E. C. Wanat, B. Suman, L. D. Schmidt, *J. Catal.* **2005**, *235*, 18–27.

7 M. Fichtner, J. Mayer, D. Wolf, K. Schubert, *Ind. Chem. Res.* **2001**, *40*, 3475–3483.

8 O. Younes-Metzler, J. Johansen, S. Thorsteinsson, S. Jensen, O. Hansen, U. J. Quaade, *J. Catal.* **2006**, *241*, 74–82.

9 A. Schneider, J. Mantzaras, P. Jahnson, *Chem. Eng. Sci.* **2006**, *61*, 4634–4649.

10 S. Hannemann, J. D. Grunwaldt, N. van Vegten, A. Baiker, P. Boye, C. G. Schroer, *Catal. Today* **2006**, *126*, 54–63.

11 I. Aartun, H. J. Venvik, A. Holmen, P. Pfeifer, O. Görke, K. Schubert, *Catal. Today* **2005**, *110*, 98–107.

12 I. Aartun, T. Gjervan, H. J. Venvik, O. Görke, P. Pfeifer, M. Fathi, A. Holmen, K. Schubert, *Chem. Eng. J.* **2004**, *101*, 93–99.

13 B. Silberova, H. J. Venvik, A. Holmen, *Catal. Today* **2005**, *99*, 69–76.

14 B. Silberova, H. J. Venvik, J. C. Walmsley, A. Holmen, *Catal. Today* **2005**, *100*, 457–462.

15 L. D. Schmidt, E. J. Klein, C. A. Leclerc, J. J. Krummenacher, K. N. West, *Chem. Eng. Sci.* **2003**, *58*, 1037–1041.

16 R. Subramanian, G. J. Panuccio, J. J. Krummenacher, I. C. Lee, L. D. Schmidt, *Chem. Eng. Sci.* **2004**, *59*, 5501–5507.

17 J. J. Krummenacher, L. D. Schmidt, *J. Catal.* **2004**, *222*, 429–438.

18 E. C. Wanat, B. Suman, L. D. Schmidt, *J. Catal.* **2005**, *235*, 18–27.

19 B. E. Traxel, K. L. Hohn, *Appl. Catal. A* **2003**, *244*, 129–140.

20 A. Qi, S. Wang, C. Ni, D. Wu, *Int. J. Hydrogen Energy*, **2006**, *32*(8), 981–991.

21 J.-M. Bae, S. Ahmed, R. Kumar, E. Doss, *J. Power Sources* **2005**, *139*, 91–95.

22 M. Fathi, F. Monnet, Y. Schuurman, A. Holmen, C. Mirodatos, *J. Catal.* **2000**, *190*, 439–445.

23 D. K. Zerkle, M. D. Allendorf, M. Wolf, O. Deutschmann, *J. Catal.* **2000**, *196*, 18–39.

24 A. Beretta, P. Forzatti, *Chem. Eng. J.* **2004**, *99*, 219–226.

25 R. F. Horng, H. M. Chou, C. H. Lee, H. T. Tsai, *J. Power Sources* **2006**, *161*, 1225–1233.

26 L. V. Mattos, F. B. Noronha, *J. Power Sources* **2005**, *152*, 50–59.

27 O. Younes-Metzler, J. Svagin, S. Jensen, C. H. Christensen, O. Hansen, U. Quaade, *Appl. Catal. A* **2005**, *284*, 5–10.

28 D. K. Liguras, K. Goundani, X. E. Verykios, *Int. J. Hydrogen Energy* **2004**. *29*. 419–427.

29 D. K. Liguras, K. Goundani, X. E. Verykios, *J. Power Sources* **2004**, *130*, 30–37.

30 A. R. Tadd, B. D. Gould, J. W. Schwank, *Catal. Today* **2005**, *110*, 68–75.

31 B. N. T. Nguyen, C. A. Leclerc, *J. Power Sources*, **2006**, *163*(2), 623–629.

32 Z. Wang, J. Xi, W. Wang, G. Lu, *J. Mol. Catal. A* **2003**, *191*, 123–134.

33 B. Lindström, J. Agrell, L. J. Pettersson, *Chem. Eng. J.* **2003**, *93*, 91–101.

34 C. Horny, L. Kiwi-Minsker, A. Renken, *Chem. Eng. J.* **2004**, *101*, 3–9.

35 M. Schuessler, M. Portscher, U. Limbeck, *Catal. Today* **2003**, *79–80*, 511–520.

36 G. Chen, S. Li, Q. Yuan, *Catal. Today* **2007**, *120*, 63–70.

37 M. L. Cubeiro, J. L. G. Fierro, *Appl. Catal. A* **1998**, *168*, 307–322.

38 J. Agrell, G. Germani, S. G. Järås, M. Boutonnet, *Appl. Catal. A* **2003**, *242*, 233–245.

39 P. Pfeifer, K. Schubert, M. A. Liauw, G. Emig, *Appl. Catal. A* **2004**, *270*, 165–175.

40 I. Aartun, B. Silberova, H. J. Venvik, P. Pfeifer, O. Görke, K. Schubert, A. Holmen, *Catal. Today* **2005**, *105*, 469–478.

41 M. Lyubovsky, H. Karim, P. Menacherry, S. Boorse, R. LaPierre, W. C. Pfefferle, S. Roychoudhury, *Catal. Today* **2003**, *83*, 183–197.

42 K. Haas-Santo, M. Fichtner, K. Schubert, *Appl. Catal. A* **2001**, *220*, 79–92.

43 C. J. Brinker, G. W. Scherer, *Sol–Gel Science*, Academic Press, San Diego, CA, Chapter 9, Figure 60.

44 C. M. Mitchell, P. J. A. Kenis, *Lab Chip* **2006**, *6*, 1328–1337.

45 R. S. Dhamrat, J. L. Ellzey, *Combust. Flame* **2006**, *144*, 698–709.

46 A. Y. Tonkovich, S. Perry, Y. Wang, D. Qiu, T. LaPlante, W. A. Rogers, *Chem. Eng. Sci.* **2004**, *59*, 4819–4824.

47 P. Pfeifer, L. Bohn, K. Haas-Santo, O. Görke, K. Schubert, *Chem. Eng. Technol.* **2005**, *28*, 474–476.

48 M. Lyubovsky, S. Roychoudhury, *Appl. Cat.al B* **2004**, *54*, 203–215.

49 G. Kolb, H. Pennemann, R. Zapf, V. Hessel, H. Löwe, in *Abstracts of 9th International Conference on Microreaction Technology*, **2008**, *135*, SUP 1, 66–73.